INSTITUTE FOR FUSION STUDIES

Laser Wakefield Excitation and Measurement by Femtosecond Longitudinal Interferometry

C.W. SIDERS, S.P. LeBLANC, D. FISHER, T. TAJIMA, M.C. DOWNER
Department of Physics
The University of Texas at Austin
Austin, Texas 78712 USA
and
A. BABINE, A. STEPANOV, and A. SERGEEV
The Institute of Applied Physics
Nizhny Novgorod, Russia

April 1996

THE UNIVERSITY OF TEXAS

AUSTIN

Laser wakefield excitation and measurement by femtosecond longitudinal interferometry

C.W. Siders, S.P. Le Blanc, D. Fisher, T. Tajima, and M.C. Downer

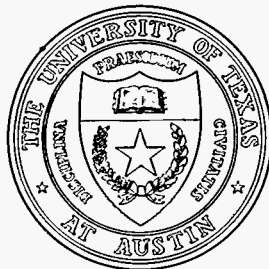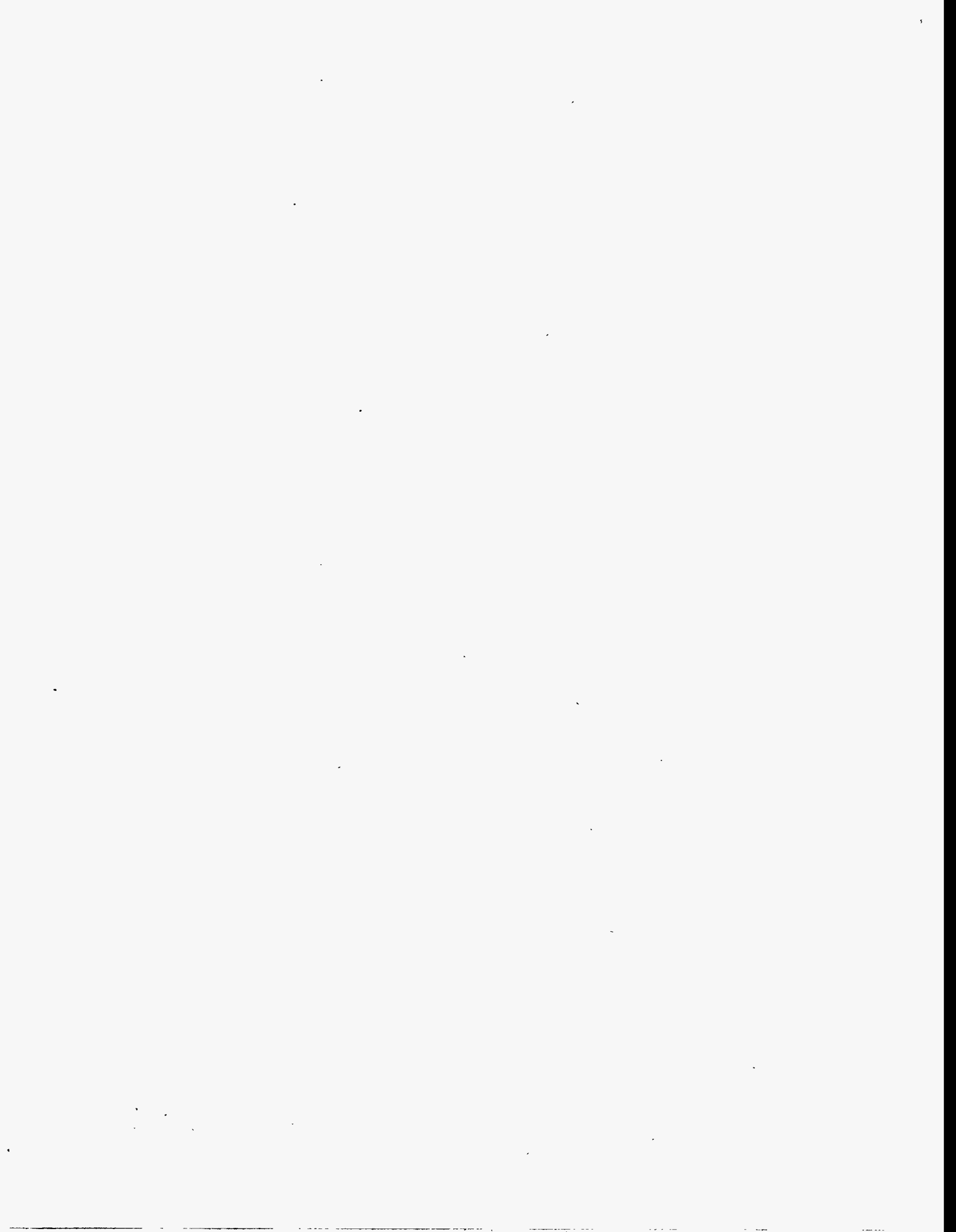*Department of Physics, The University of Texas at Austin, Austin, Texas 78712 USA*

and

A. Babine, A. Stepanov, and A. Sergeev

The Institute of Applied Physics, Nizhny Novgorod, Russia

Abstract

Plasma density oscillations (Langmuir waves) in the wake of an intense ($I_{peak} \sim 3 \times 10^{17} W/cm^2$) laser pulse (100 fs) are measured with ultrafast time resolution using a longitudinal interferometric technique. Phase shifts consistent with large amplitude ($\delta n_e/n_e \sim 1$) density waves at the electron plasma frequency were observed in a fully tunnel-ionized He plasma, corresponding to longitudinal electric fields of ~ 10 GV/m. Strong radial ponderomotive forces enhance the density oscillations.

Because the immense electrostatic fields present in large amplitude Langmuir plasma waves can approach atomic scale values ($E_a \sim 500\,\mathrm{GV/m}$) which far exceed those achievable in conventional accelerators, plasma based accelerators have received considerable attention as compact sources of high-energy electron pulses.[1,2] To date, externally injected electrons have been accelerated by up to tens of MeV in Langmuir waves generated by the ponderomotive force of two temporally beating laser pulses,[3] by the ponderomotive force of a single short laser pulse,[5] and by the Coulomb force of an electron pulse.[4] Except in the case of quite long wavelength ($\lambda_p \sim 1\mathrm{cm}$) wakefields,[4] however, observation of acceleration products provides only indirect information on the transverse and longitudinal microstructure of the plasma wave itself. Detailed mapping of short wavelength ($\lambda_p \sim 100\mu\mathrm{m}$), high gradient ($E \gtrsim 1\,\mathrm{GV/m}$) plasma waves requires high longitudinal resolution available only from ultrashort optical pulses. Optical probes such as stimulated Raman scattering or terahertz radiation at the electron plasma frequency ω_p[6] have provided only spatially averaged indications of the wave's existence. In this Letter, we report femtosecond time resolved measurements of the longitudinal and radial structure of laser induced wakefield oscillations using an all optical technique known as photon acceleration.[7] The ability to measure the plasma wake microstructure directly is important for addressing several fundamental issues: wakefield generation by optimized pulse trains,[8] design of particle injectors synchronized to the laser pulse on a femtosecond time scale, growth dynamics of plasma wave instabilities.[5] and self-consistent propagation of laser pulse and wake in plasma channels.[9]

For wakefields generated by tightly focused laser pulses, both longitudinal and radial ponderomotive forces contribute to plasma wave excitation. Below the wavebreaking limit, these contributions are well described by a second order perturbative solution of the 2D nonrelativistic cold fluid equations.[10] For a radially Gaussian laser pulse of longitudinal shape $f(\zeta)$ described by the normalized vector potential $a^2(\zeta, r) = a_0^2 f(\zeta)e^{-(r/\sigma_r)^2}$, the density

2

oscillations $n_e(\zeta, r) = n_{e0} + \delta n_e(\zeta, r)$ are

$$\frac{\delta n_e}{n_{e0}} = \frac{a_0^2}{2} e^{-(r/\sigma_r)^2} \left[1 + \frac{4}{(k_p \sigma_r)^2} \left[1 - (r/\sigma_r)^2 \right] \right] \times$$

$$\sqrt{2\pi} \left[|k \, \mathrm{FT} \{ f(\zeta) \}|^2 \right]_{k=k_p}^{1/2} \sin \left[k_p \zeta + \arg \left[\mathrm{FT} \{ f(\zeta) \} \right] \right], \tag{1}$$

where $\zeta = z - ct$, $k_p = \omega_p/c$, FT denotes Fourier transform, and the factor $|k \, \mathrm{FT} \{ f(\zeta) \}|^2_{k=k_p}$, which determines the longitudinal resonance condition $\omega_p \tau = \kappa \pi$, is determined experimentally from the second order autocorrelation of the pulse. For a longitudinally Gaussian pulse $f(\zeta) = e^{-(\zeta/\sigma_z)^2}$, the second line of Eq. (1) simplifies to $\sqrt{\pi} \, k_p \sigma_z e^{-(k_p \sigma_z)^2/4} \sin k_p \zeta$, with maximum at $\kappa = (2/\pi)\sqrt{2 \ln 2}$. For a 1D experiment ($k_p \sigma_r \gg 1$) generation of large amplitude ($0.1 \lesssim \delta n_e/n_{e0} \lesssim 1.0$) density oscillations requires high intensity $a_0 \sim 1$, near resonant conditions. For a 2D experiment ($k_p \sigma_r \lesssim 1$), on the other hand, the radial ponderomotive force enhances the density oscillations, thus relaxing the requirements on a_0 and limiting the pulse energy which can be used without exciting extremely nonlinear plasma waves ($\delta n_e \gtrsim n_{e0}$). Laser-driven wakefields in a plasma were first detected in such an extreme 2D regime ($k_p \sigma_r \lesssim 0.1$) by observations of far-infrared radiation.[6] In the experiments described herein, the electron density oscillation is probed via shifts in optical phase which it induces on a weak ultrashort laser pulse which copropagates with the pump. For Gaussian pump and probe pulses Eq. (1 can be averaged radially and integrated longitudinally to yield the maximum phase shift relative to propagation in vacuum:

$$\Delta \phi = \frac{r_e k_p}{2\sqrt{\pi}} \frac{E}{m_e c^2} \frac{\lambda^2}{\sigma_{r0}^2} e^{-(k_p \sigma_z)^2/4} \left(1 + (k_p \sigma_{r0})^2 \right), \tag{2}$$

where E is the laser pump pulse energy, σ_{r0} is the common pump and probe beam radius in the focus, r_e is the classical electron radius, and $m_e c^2$ is the electron rest energy. Clearly measurements of $\Delta \phi$ will resolve plasma wave features of length scales $\gtrsim \sigma_{r0}$, σ_z but will significantly average smaller features. Note that $\Delta \phi$ is maximum when $k_p \sigma_z = \sqrt{2}$ in the 2D

3

regime ($k_p \sigma_{r_0} < 1$), while for the 1D regime, $k_p \sigma_z = \sqrt{6}$. Equation (2) is strictly valid only for $\delta n_e(E, \sigma_z, \sigma_{r_0}, k_p) \leq n_{e0}$.

The experimental setup for our interferometric photon accelerator is described in detail elsewhere.[11] Only key points are summarized here. A Ti:Sapphire laser system based on chirped pulse amplification and capable of delivering 20 mJ, 100 fs, laser pulses at 30 Hz and $\lambda = 0.8\mu$m generated linearly polarized pump and multiple orthogonally polarized probe pulses for the experiment.[11] These copropagating, temporally separated pulses are focused and recollimated by $f = 5$cm off-axis parabolic mirrors in a background of 2-12 Torr helium gas. The pump and probe pulses focus to a spot size of 3.6μm (e^{-1} intensity radius) over a Rayleigh length of 52μm, yielding a peak pump intensity of $4.5 \times 10^{17}\,$Wcm^2 and a fully ionized helium plasma over a length more than 500μm. As the pump pulse ionizes the gas and exerts ponderomotive pressure on the resulting plasma, a plasma wave is excited which propagates with phase velocity equal to the group velocity of the laser pulses. Thus each probe pulse samples a portion of the copropagating plasma density wave $n_e(\zeta, r)$ about a point (ζ, r) and experiences an optical phase shift $\Delta\phi$ and spectral shift $\Delta\omega$[12] proportional to $n_e(\zeta, r)$ and $\partial n_e(\zeta, r)/\partial\zeta$, respectively. By using one probe pulse which precedes the pump, and therefore is unaffected by ionization or wakefield generation, and one or more after the pump, both n_e and its derivative for multiple points in the plasma wave can be recorded in frequency-domain interferograms..[11,13] Alternatively, relative values of n_e within the plasma wave can be recorded by interfering two probes after the pump. In order for the pump and probe beams to maintain overlap in the focus, their angular separation is held to within $\theta \sim 150\mu$rad by a piezoelectrically controlled mirror mount.[11] The frequency domain interference spectra of the probe pulses which traversed the plasma wave as well as an identical probe sequence which bypassed the plasma are recorded simultaneously by a $f = 275\,$mm focal length spectrometer equipped with a dual photodiode array. Using laser pulse energy monitors, data acquisition can be limited in real time to a specified pulse energy

4

window (typically 2-4%).

Two types of experiments were conducted, both utilizing two probe pulses and one pump pulse. In the first experiment, the delay of the pump pulse was varied relative to the two probe pulses. This time delay scan was conducted at a constant gas pressure chosen to be nearly resonant ($n_{res} = 3.1 \times 10^{21} \text{cm}^{-3} \, \kappa^2/\tau^2 \text{[fs]}$) yet allow good temporal resolution with a FWHM laser pulse duration τ. Figure 1 shows measured wakefield oscillations in 4.8 (2.7) Torr helium ($n_{e0} = 3(1.7) \times 10^{17} \text{cm}^{-3}$). For 4.8 Torr, the probe pulse separation was fixed at 2.2 ps. The 10 mJ pump pulse was positioned 550 fs in front of the second probe pulse and scanned away from it in steps of 13.3 fs. For the 2.7 Torr data, the probe pulse separation was fixed at one and one half plasma periods and both pulses traveled behind the pump. Each data point in Fig. 1 represents the phase difference $\Delta\phi$ of a 100 shot average with and without the pump with $\pm\sigma$ error bars. To indicate the level of noise in the data, the top line of data points in Fig. 1 shows an identical delay scan conducted in an evacuated chamber. An essentially identical null scan is obtained with pump and probe beam waists misaligned by more than σ_{r0} in a gas-filled chamber. The middle set of data points in Fig. 1 shows $\Delta\phi$ oscillating about a DC phase shift of 0.15 rad with a period of 220 ± 25 fs and an amplitude of 7 mrad, to be compared with an estimate from Eq. (2) of ~ 10 mrad. The bottom set of data points shows the phase shift oscillating with period 270 ± 10 fs and slightly less amplitude. The time scans resolve the third to fifth wakefield oscillation for the 4.8 Torr data and the fourth to fifth oscillation for the 2.7 Torr data. The phase and frequency of the wakefield oscillations are consistent with numerical models. In the linear regime, the wakefield period is given by $T_p = 2\pi/\omega_p = 200(267)$ fs and is determined solely by the plasma density. Several nonlinear effects tend to cause the plasma frequency, especially in the central focal region, to deviate from ω_p. These include relativistic electron mass increase,[2] higher-order self-generated magnetic and electrostatic effects,[14] with the first two lengthening the period and the last shortening it (thermal effects are negligible with our cold field-ionized

5

plasma). Estimates of peak electron fluid velocities ($(v/c)^2 \lesssim 2.5\%$) suggest that relativistic nonlinearities are not insignificant, while electrostatic and magnetic nonlinearities should not exceed 10%.[14] As these effects will occur only in the central focus, longitudinal averaging further reduces the effects of these nonlinear ω_p shifts on the observed $\Delta\phi(t)$. From nonlinear least square fits to the data, we find that the observed oscillation periods are consistent with both the linear and slightly lengthened ($\lesssim 10\%$) values. From the measured $\Delta\phi$ in Fig. 1 and taking into account the focal geometry, we estimate maximum density variations of $\delta n/n = 0.8$ in the focus. A simple one (longitudinal) dimensional theory predicts only $\delta n/n \sim 0.025$ for our conditions. The 2D theory (Eq. 1), on the other hand, predicts $\delta n/n \sim 1$ in our focus ($k_p \sigma_{r_0} = 0.4$), in good agreement with the experiment, because the radial ponderomotive force is about ten times larger than the axial component. The peak longitudinal electric field corresponding to these density oscillations is ~ 10 GV/m.

A second set of experiments was conducted by fixing the pump and probe pulse delays while varying the helium gas pressure. Such a pressure scan allows the wakefield to be scanned across the probe pulse sequence without spurious effects from delay-stage motion and is equivalent to the time scan measurement except for three factors. First, increasing the pressure decreases T_p; consequently, temporal resolution is reduced at higher pressures. Secondly, the amplitude of the wakefield maximizes at the resonant pressure ($k_p \sigma_z = \sqrt{2}$) and falls off slowly at higher and lower pressures. Lastly, the overall DC phase shift from the ambient plasma monotonically increases with pressure and must be subtracted from the data to reveal the wakefield oscillations. Figure 2a shows the measured $\Delta\phi$ for pump intensities of 7.5×10^{16} W/cm^2 (2.5 mJ) and 3×10^{17} W/cm^2 (10 mJ) as the He pressure varied from 2-12 Torr.

The detected $\Delta\phi$ in Fig. 2a becomes positive or negative depending on the phase of the wakefield oscillation at the position of the second probe pulse. Although the pump pulse intensities differ by a factor of four, the detected oscillatory phase shifts remain similar,

except near and below the resonant density where they are slightly larger for the lower intensity pump pulse. For those densities, the radial enhancement of the density perturbation is expected to cause strongly nonlinear wakefield oscillations for the higher intensity pump pulse. Superimposed on the data is a calculated pressure scan of $\Delta\phi$ based on Eq. (2). Pulse-width averaging becomes important when the wakefield period approaches the probe pulse duration ($2\pi/\omega_p \sim \tau$ at $p \sim 20$ Torr). Because phase noise increases with pressure, the dashed lines in Fig. 2a indicate the range of expected phase shifts due to fluctuations in pump pulse characteristics.

To reduce radial averaging, a third pressure scan was performed with a smaller slit at the spectrometer input. The maximum $\Delta\phi$ in this pressure scan (Fig. 2b) indeed increased significantly over the oscillations in Fig. 2a, in better agreement with calculated pressure scans when only longitudinal averaging is included. The noise level in the data also increased, however, because of greater sensitivity to probe beam pointing fluctuations.

Though our use of dual-beam spectroscopy eliminates most systematic contribution to our data on a 2000:1 (long term) level, approximately 10% of the data points fall significantly away from the calculated pressure scan curves in Fig. 1 and 2. Uncorrected drifts in beam pointing, center wavelength, and spectral shape on the time scale of the data collection (~ 40 sec for each data point) have been found to contribute significantly to such noise in the data. Even so, nonlinear effects such as radial density peaking, radial dephasing and wave breaking[14] may also contribute to the data in ways which are not well understood at present.

In an effort to evaluate nonlinear contributions quantitatively, numerical simulations were performed with a 2D, multi-grid, fully relativistic, cold fluid model in which a Gaussian laser pulse propagates through a preformed plasma. The $\mathbf{v} \times \mathbf{B}$ term of the Lorentz force was not included; thus only relativistic and electrostatic influences on ω_p were modeled. Figure 3 shows the calculated resonantly excited wakefields for the focal geometry and pulse

energies as used in the experiment. The higher energy simulation (Fig. 3a) clearly shows the excitation of nonlinear plasma waves with significant density peaking and a maximum $\delta n/n \sim 5$. Even in the intense focus, these plasma waves oscillate for at least five cycles after the pump pulse. The lower energy simulation (Fig. 3b) shows significantly reduced peaking with $\delta n/n \sim 1$, in agreement with the analytic solution (Eq. (1). Careful examination showed that the higher energy simulation has a period longer than either the lower energy simulation or the linear result in the focus, suggesting that relativistic period lengthening dominates over electrostatic period shortening. For our parameters, then, we expect only slight (a few percent) period lengthening and then only in the most intense portion of the focus, consistent with the observed wakefield periods.

Numerical integration of the data in Fig. 3 confirms that for our focal geometry and pulse widths $\Delta\phi \sim 10$ mrad is expected for both 2.5 mJ and 10 mJ pump energy, consistent with the data in Fig. 2a and with the predictions of Eqs. (1) and 2 ($\delta n/n \sim 1, \Delta\phi \sim 10\,\text{mrad}$) for the 2.5 mJ pump. The sharply peaked density perturbation in Fig. 3a does not result in a larger measured $\Delta\phi$ than the broader, lower peak in Fig. 3b because the high electron density is concentrated in a volume smaller than the probe pulse, and thus is not resolved in our data.

In summary, we have used longitudinal pump-probe interferometry to measure near-resonantly excited laser wakefield oscillations with femtosecond resolution in both time-delay and pressure scan configurations. From the data, we estimate relative density perturbations of order unity and longitudinal fields of order 10 GV/m, consistent with the predictions of both analytic 2D linear nonrelativistic fluid analysis and fully relativistic nonlinear 2D self-consistent numerical modeling. By using tightly focused laser pulses, nonlinear wakefield oscillations were driven with subrelativistic laser intensity ($I < 10^{18}\text{W/cm}^2$). As this technique utilizes a necessary component of any laser-based plasma accelerator, i.e. the intense driving pulse, it promises to be a powerful tool for on-line monitoring and control of future

8

plasma based particle accelerators.

Acknowledgments

REFERENCES

[1]T. Tajima and J.M. Dawson, Phys. Rev. Lett. **43**, 267 (1979); J.S. Wurtele, Phys. Today, 33 (July 1994).

[2]P. Sprangle and E. Esaray, Phys. Fluids B 4, 2241 (1992).

[3]C.E. Clayton *et al.*, Phys. Rev. Lett. **54**, 2343 (1985).

[4]J.B. Rosenzweig *et al.*, Phys. Rev. Lett. **61**, 98 (1988).

[5]K. Nakajima *et al.*, Phys. Rev. Lett. **74**, 4428 (1995); A. Modena *et al.*, Nature **377**, 606 (1995).

[6]H. Hamster *et al.*, Phys. Rev. A **49**, 671 (1994).

[7]S.C. Wilks *et al.*, Phys. Rev. Lett. **62**, 2600 (1989);

[8]D. Umstadter *et al.*, Phys. Rev. Lett. **72**, 1224 (1994).

[9]C.G. Durfee III *et al.*, Phys. Rev. Lett. **71**, 2409 (1993); W. Leemans *et al.*, IEEE Trans. Plasma Sci. (in press); T.C. Chiou *et al.*, Phys. Plasmas **2**, 310 (1995).

[10]E. Esarey *et al.*, Comments Plasma Phys. Control. Fusion **12**, 191 (1989); L.M. Gorbunov *et al.*, Sov. Phys. JETP **66**, 290 (1987).

[11]C.W. Siders *et al.*, IEEE Trans. Plasma Sci. (in press); C.W. Siders *et al.*, Rev. Sci. Instr. **65**, 3140 (1994).

[12]W.M. Wood *et al.*, Phys. Rev. Lett. **67**, 3523 (1991); C.W. Siders *et al.*, J. Opt. Soc. Am. B **13**, 330 (1996).

[13]C. Froehly *et al.*, J. Opt. (Paris) **4**, 183 (1973); F. Reynaud *et al.*, Opt. Lett. **14**, 275 (1989); E. Tokunaga *et al.*, Opt. Lett. **17**, 1131 (1992); J.P. Geindre *et al.*, Opt. Lett. **19**, 1997 (1994).
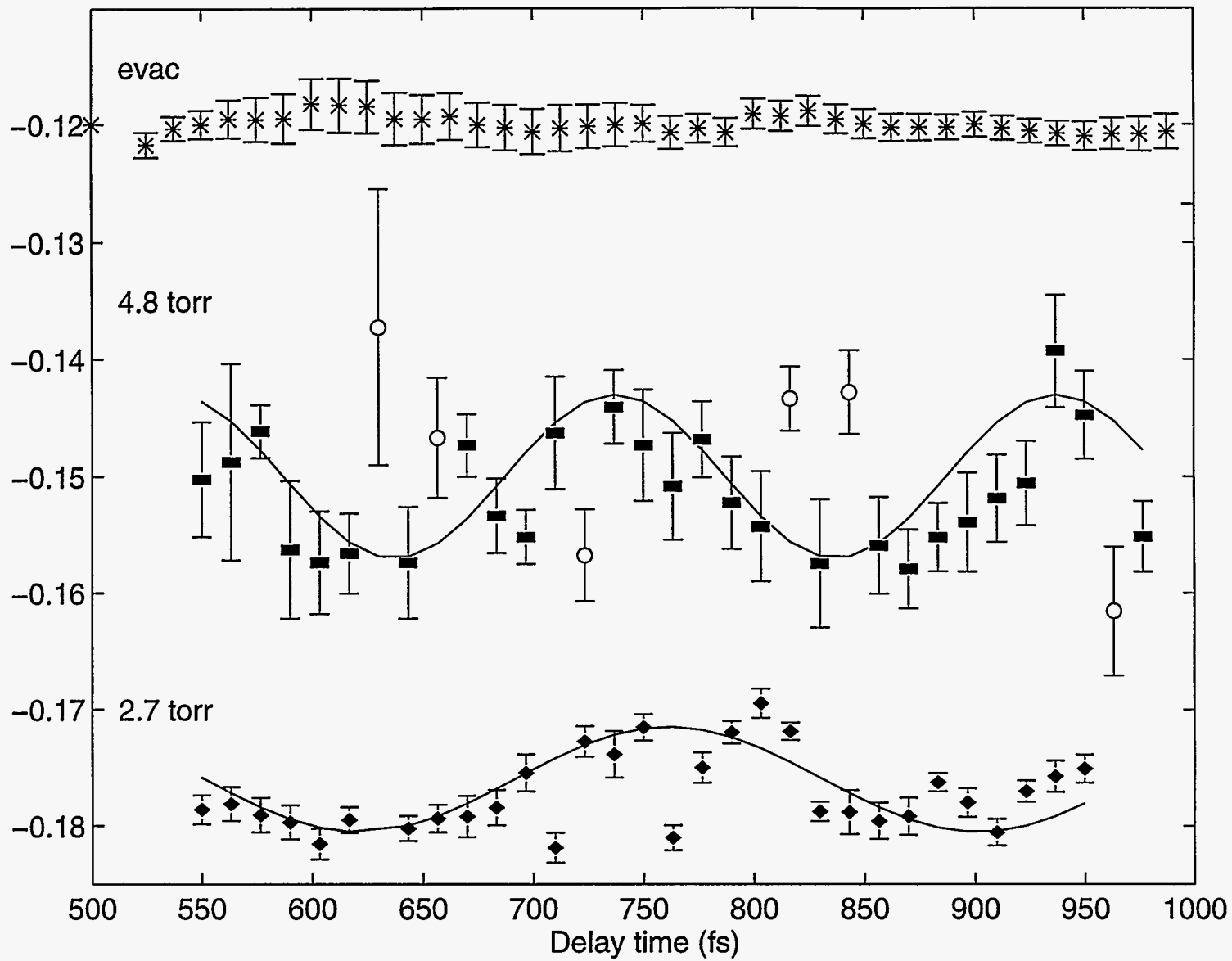
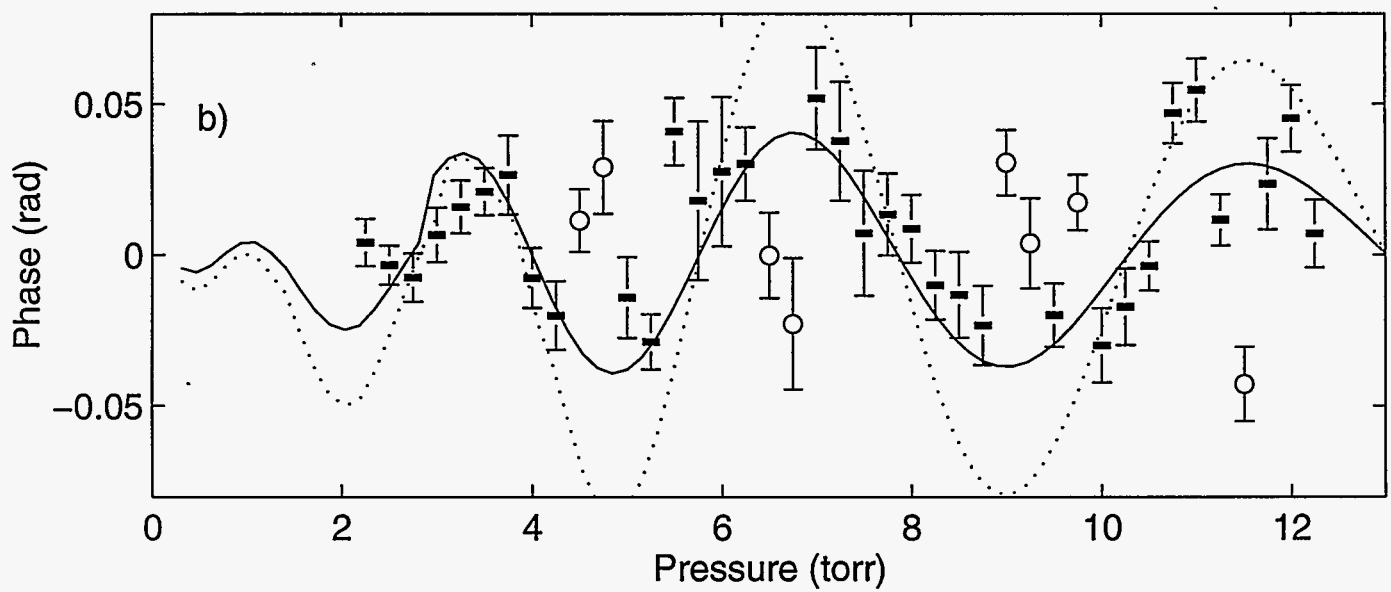[14]J.M. Dawson, Phys. Rev. **113**, 383 (1959); A.R. Bell *et al.*, Plasma Phys. Control. Fusion **30**, 1319 (1988).
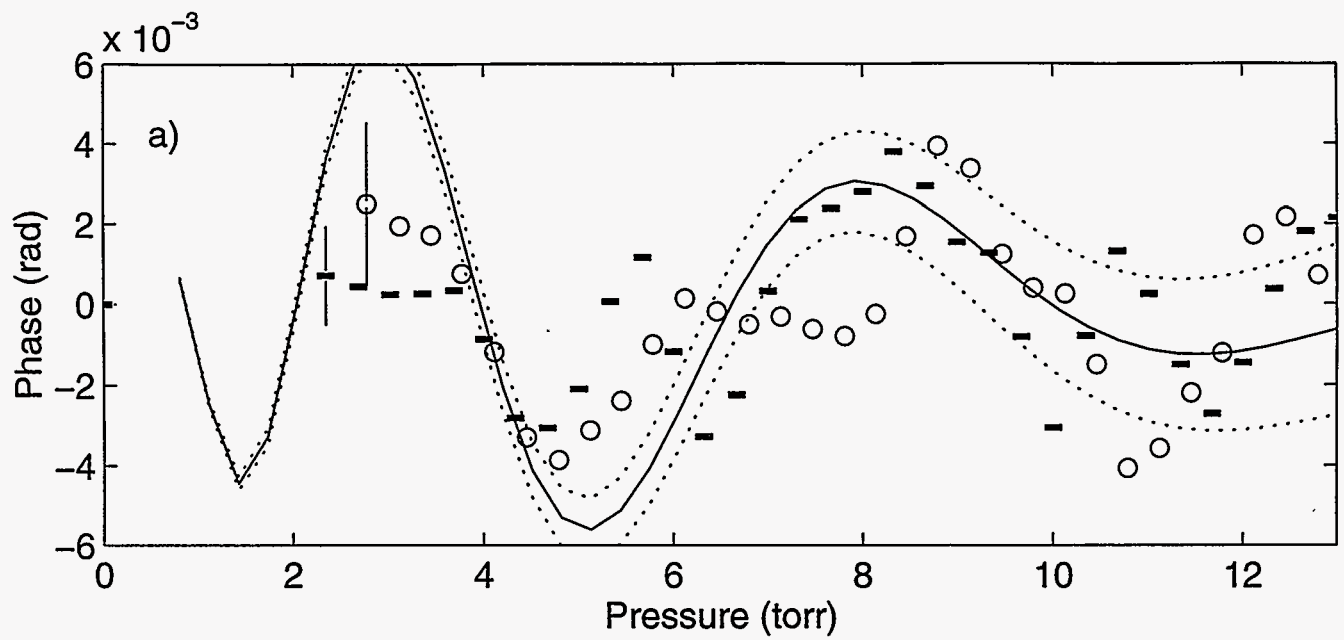
FIGURE CAPTIONS

FIG. 1. Measured wakefield oscillations in helium. For the 4.8 Torr data, the two probe pulses are separated by 2.2 ps about the pump, while in the 2.7 Torr data (offset from zero and shifted by -400 fs) the probes trail the pump with 415 fs separation. For the 4.8 (2.7) Torr data, 10 (9) mJ of energy was focused with an e^{-1} radius of 3.6 (5.0) μm, as confirmed by appearance energy measurements. The solid lines show the calculated phase shift due to the wakefield oscillations. Evacuated chamber data is shown offset from zero.
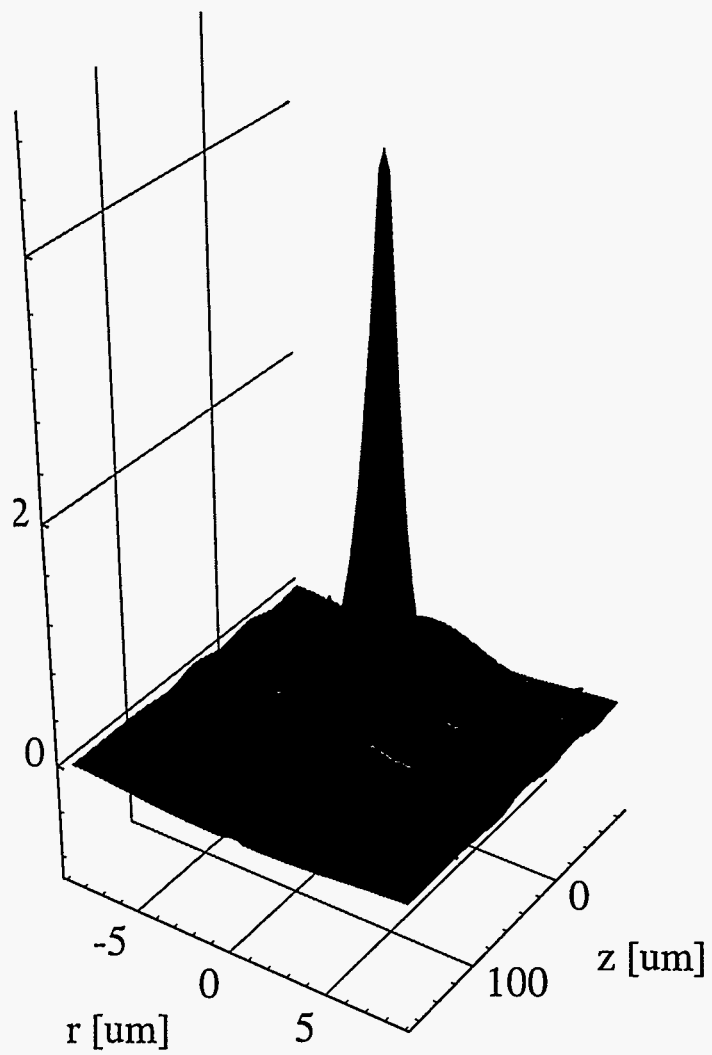
FIG. 2. Phase shift as a function of He gas pressure. (a) For two pulse energies: 10 mJ (filled square) and 2.5 mJ (circle). The solid line indicates a calculation of $\Delta\phi$ for the higher energy. Representative error bars shown. (b) Pressure scan (10 mJ) with narrow slit to reduce radial averaging. Curves are theoretical calculations of the phase shift without (dotted line) and with (solid line) radial averaging.

FIG. 3. Two dimensional numerical simulation of wakefield oscillations $\delta n_e/n_e$ corresponding to 3.6μm spot radius, $\tau = 100$ fs, $n_e = 3\times10^{17}$cm^{-3}). These panels show the electron density oscillations within the confocal parameter of the tightly focused pump pulse (centered at $z = 111\mu$m and moving in the positive z direction, but not shown). The heavy lines represents the e^{-1} focal contours of the laser intensity.

a)

b)

a) E = 10 mJ   b) E = 2.5 mJ